JACS
JOURNAL OF THE AMERICAN CHEMICAL SOCIETY
Article
pubs.acs.org/JACS

Origin of Stereocontrol in Guanidine-Bisurea Bifunctional Organocatalyst That Promotes α-Hydroxylation of Tetralone-Derived β-Ketoesters: Asymmetric Synthesis of β- and γ-Substituted Tetralone Derivatives via Organocatalytic Oxidative Kinetic Resolution

Minami Odagi,[†] Kota Furukori,[†] Yoshiharu Yamamoto,[†] Makoto Sato,[‡] Keisuke Iida,[†] Masahiro Yamanaka,[‡] and Kazuo Nagasawa*[,†]

[†]Department of Biotechnology and Life Science, Tokyo University of Agriculture and Technology, 2-24-16, Naka-cho, Koganei city, 184-8588, Tokyo Japan

[‡]Department of Chemistry, Faculty of Science, Rikkyo University, 3-34-1 Nishi-Ikebukuro, Toshima-ku, 171-8501, Tokyo Japan

Supporting Information

ABSTRACT: The mechanism of asymmetric α-hydroxylation of tetralone-derived β-ketoesters with guanidine-bisurea bifunctional organocatalyst in the presence of cumene hydroperoxide (CHP) was examined by means of DFT calculations to understand the origin of the stereocontrol in the reaction. The identified transition-state model was utilized to design an enantioselective synthesis of β- or γ-substituted tetralones by catalytic oxidative kinetic resolution reaction of tetralone-derived β-ketoesters. This kinetic resolution reaction proceeded with high selectivity, and selectivity factors (*s* value) of up to 99 were obtained. The potential utility of this oxidative kinetic resolution method for synthesis of natural products was confirmed by applying it to achieve an enantioselective synthesis of (+)-linoxepin (**13**) from β-substituted tetralone *rac*-**7** in only six steps.

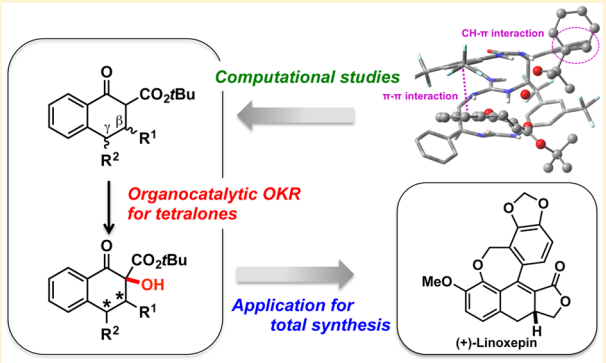

INTRODUCTION

We have developed a series of guanidine-bis(thio)urea bifunctional compounds **1** and **2** as organocatalysts[1] and have employed them for Henry reaction,[1a] aza-Henry reaction,[1d] Mannich-type reaction,[1e,g] and Friedel–Crafts reaction[1f,h,i] (Scheme 1a). Even though these catalysts have flexible linear structure, high enantioselectivities were obtained. In structure–activity relationship studies, we found that the bifunctionality and pseudo-C_2 symmetrical structure of **1** and **2** were mandatory for high selectivity. We proposed that these catalytic reactions involve interactions of the guanidine moiety with nucleophiles and the (thio)urea moiety with electrophiles (Scheme 1a).

We recently developed an α-hydroxylation reaction of tetralone-derived β-ketoesters **3** with cumene hydroperoxide (CHP) in the presence of guanidine-bisurea bifunctional organocatalyst **2d** (Scheme 1b).[2] In this reaction, interactions between guanidine and β-ketoester and between the urea group and CHP appeared to be important for high enantioselectivity. However, the roles of these functional groups and the influence of the characteristic linear structures of the catalysts, including the necessity of pseudo-C_2 symmetric structure, remained unclear. We herein carried out DFT calculations to obtain mechanistic insight into this organocatalytic reaction. We identified a transition-state (TS) model that reasonably explained the roles of the three functional groups, i.e., one guanidine and two urea groups, in the catalyst **2**.[3] Further consideration of this TS model led us to design an oxidative kinetic resolution reaction of β- or γ-substituted tetralone-derived β-ketoesters *rac*-**5** (Scheme 1c). In this reaction, we found that corresponding β- and γ-substituted tetralones were obtained with high enantioselectivity. Since there are few methods for asymmetric synthesis of β- and γ-substituted tetralones, mainly because of the instability of the precursors, the present method should be practically useful for obtaining chiral β- and γ-substituted tetralones. To confirm its utility, we applied this method to a short synthesis of (+)-linoxepin (**13**), which contains a β-substituted tetralone structure.

RESULTS AND DISCUSSION

DFT Calculation of α-Hydroxylation of Tetralone-Derived β-Ketoesters Catalyzed by Guanidine-Bisurea Bifunctional Organocatalyst. Transition structures for the α-hydroxylation reaction of β-ketoester **3** catalyzed by **2d** were explored to elucidate the origin of the stereocontrol. Geometry optimization and frequency analysis were performed by B3LYP[4]

Received: November 4, 2014
Published: January 12, 2015

DOI: 10.1021/ja511149y
J. Am. Chem. Soc. 2015, 137, 1909–1915

Scheme 1

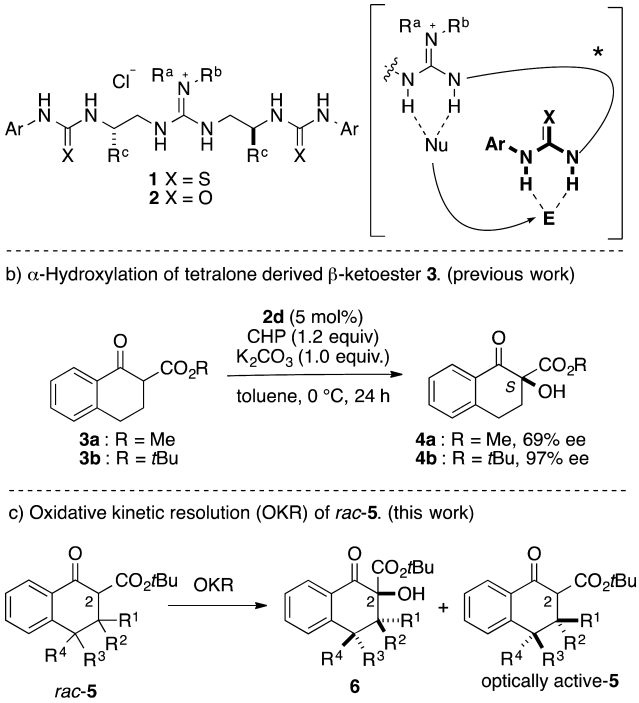

[a]Structure of guanidine-bis(thio)urea bifunctional organocatalysts **1** and **2**, and a plausible model of the interaction with nucleophiles and electrophiles. [b]Previous α-hydroxylation of β-ketoesters **3** catalyzed by **2d**. [c]Oxidative kinetic resolution reaction of *rac*-**5** explored in this study.

and M05-2X[5] functionals with the 6-31G* basis set[6] using the Gaussian 09 program.[7] Thermodynamic properties were estimated at 298.15 K at 1 atm. Various TS conformations and activation modes in the α-hydroxylation of β-ketoester **3** catalyzed by **2d** were explored using simplified chemical models at the B3LYP/6-31G* level.[8] Pseudo-C_2 symmetric catalyst structures, in which the guanidinium and the urea groups activate β-ketoester enolate and oxidant, respectively, through hydrogen bonds, were found to be relatively stable. Next, M05-2X/6-31G* calculation was applied to take into account dispersion interactions such as π−π and CH−π interactions of the Ar groups in realistic chemical models (R^1 = Me, R^2 = H, R^3 = Ph, and Ar = 3,5-$(CF_3)_2C_6H_3$ in **2**).[9]

The identified TS models are summarized in Figure 1. The Gibbs free energy difference (Δ*G*) between **TSa-S** and **TSa-R** for **3a** (R = Me) is calculated to be 0.81 kcal mol^{-1}.[10] When the ester substituent of the β-ketoester enolate is changed from methyl to *t*-butyl, i.e., **3b** (R = *t*-Bu), Δ*G* between **TSb-S** and **TSb-R** becomes larger, reaching 2.49 kcal mol^{-1}. These results are consistent with the experimental findings that the *S*-form is obtained as the major product and higher selectivity is observed in the case of **3b** (Scheme 1b). The diasteromeric TS models for **3a** (**TSa**: R = Me) and **3b** (**TSb**: R = *t*-Bu) both have the guanidinium-bisurea catalyst in a pseudo-C_2 symmetric structure, coordinating with the β-ketoester and oxidant through the following interactions: (1) hydrogen-bonding interaction between guanidinium NH and F of the 3,5-$(CF_3)_2C_6H_3$ group and (2) attractive dispersion interactions of the aromatic rings (Figure 1). In these TS models, four NH residues in the guanidinium (NH_{gua}) and urea groups (NH_{ure}) coordinate to two carbonyl groups in the β-ketoester enolate **3**, and these interactions play crucial roles in controlling the orientation of the β-ketoester enolate.[11] Moreover, the remaining two NH_{ure} of the urea group activate cumene hydroperoxide (CHP) through hydrogen-bonding interaction with oxygen attached to the carbon in cumene. These comprehensive intra/intermolecular interactions construct the compact chiral reaction field through induced-fit-type structural changes.

The distortion/interaction analysis[12] of these diastereomeric TS models indicated that two factors mainly contribute to the stabilization of **TS-S**. The first factor is the intra- and intermolecular attractive interaction modes (e.g., hydrogen-bonding, π−π, and CH−π interactions). The hydrogen-bonding networks around the β-ketoester enolate are much differentiated between **TSa-S** and **TSa-R**. In the case of **TSa-S**, three NH residues, i.e., two NH_{gua} and one NH_{ure}, interact with the ketone carbonyl (CO_{ket}). In the case of **TSa-R**, on the other hand, two NH residues (NH_{gua} and NH_{ure}) interact with the ester carbonyl (CO_{est}). Thus, **TSa-S** having the larger number of hydrogen-bonding interactions is more effectively stabilized than **TSa-R** due to electronically more negative CO_{ket} than CO_{est}.[13] In addition, the intramolecular CH···F hydrogen bond in the catalyst and the intermolecular π−π and CH−π interactions between the catalyst and the substrates significantly stabilize **TSa-S** (Figure 1). Whereas the intramolecular hydrogen bond in the catalyst is similar, the intermolecular dispersion interactions are slightly enhanced in **TSb-S**. The second factor is the steric repulsion between the ester group of the β-ketoester enolate and the 3,5-$(CF_3)_2C_6H_3$ group in the catalyst. The ester group in **TS-S** is oriented to the outer side of the chiral space for the reaction, and no significant steric hindrance is observed. On the other hand, the ester group in **TS-R** is embedded in the narrow space constructed by the Ar groups in the catalyst. The *t*-butyl ester group in **TSb-R** causes serious steric constraint and significantly decreases the interaction energy between the catalyst and the substrates. In addition, the 3,5-$(CF_3)_2C_6H_3$ group is pushed out to move CHP interacting with the urea moiety into an unfavorable position in **TSb-R** (Figure 1).[14] These structural changes around the urea moiety in **TSb-R** decrease the CH−π interaction between CHP and the β-ketoester enolate. Therefore, the energy difference Δ*G* between **TSb-S** and **TSb-R** becomes larger in the case of **3b** bearing *t*-butyl ester owing to destabilization of **TSb-R**.

Thus, as described above, our computational results successfully account for the highly enantioselective α-hydroxylation of tetralone-derived β-ketoesters by structurally flexible guanidine-bisurea catalyst **2**. Next, we explored whether this information could be applied to asymmetric synthesis of β- and/or γ-substituted tetralones.

Development of Oxidative Kinetic Resolution of β- and γ-Substituted Tetralone-Derived β-Ketoesters. β- and γ-Substituted carbonyl compounds are ubiquitous in natural products, as well as biologically active molecules, and several synthetic approaches, including enantioselective versions, have been reported. The most widely used approaches include asymmetric Michael reaction with α,β-unsaturated carbonyl compounds and alkylation of dienolate derived from α,β-unsaturated carbonyl compounds.[15] These strategies have been applied to a variety of α,β-unsaturated carbonyl compounds, including linear as well as cyclic molecules, but they have several limitations as regards substrates. One of the more serious restrictions applies to tetralone derivatives. Although tetralone structure is found in many biologically active molecules (Figure 2),[16] derivatization at the β- or γ-position is difficult, because the

DOI: 10.1021/ja511149y
J. Am. Chem. Soc. 2015, 137, 1909−1915

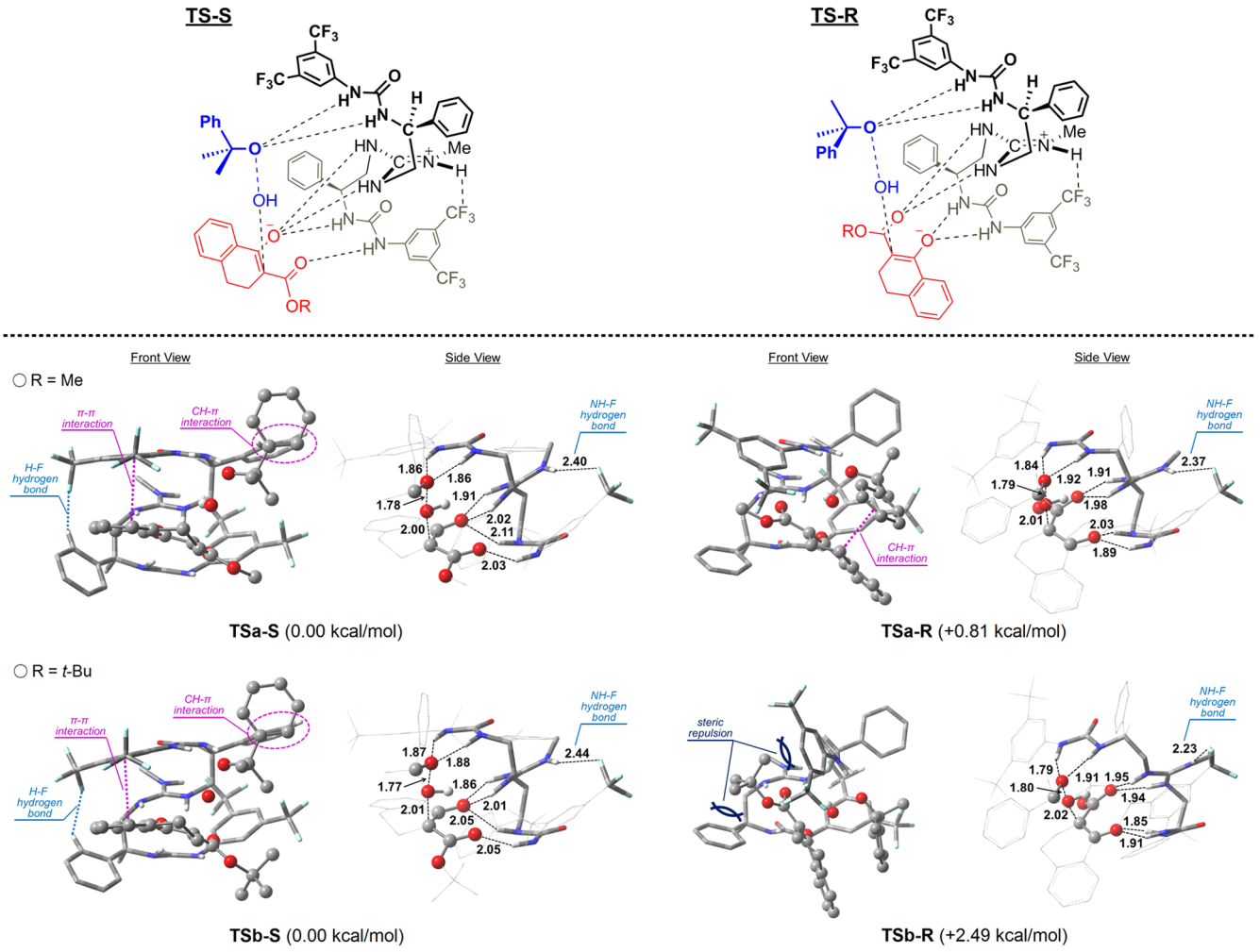

Figure 1. Schematic representations (front view) and 3D structures (bottom and side views) of **TS-S** and **TS-R** (**TSa**: R = Me, **TSb**: R = *t*-Bu) for **3**. *β*-Ketoester enolate and CHP are indicated by ball and stick models; the catalyst is shown as a tube model; unimportant hydrogen atoms are omitted. Distances are in Å.

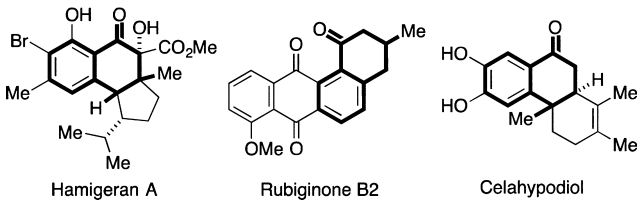

Figure 2. Representative natural products bearing *β*- and/or *γ*-substituted tetralone core structures.

Scheme 2. Functionalization of *α,β*-Unsaturated Tetralone Is Difficult Because of Its Instability

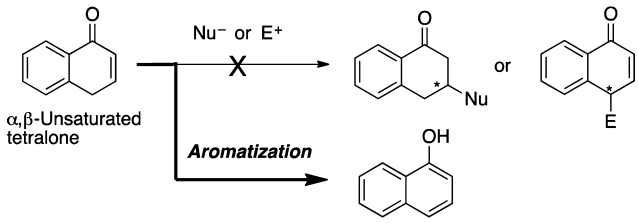

corresponding *α,β*-unsaturated carbonyl compounds are unstable and quickly aromatized (Scheme 2).[17] Therefore, new methodologies are needed for enantioselective synthesis of *β*- and/or *γ*-substituted tetralones.[18−20] A representative approach to construction of *β*- and/or *γ*-substituted tetralones involves Diels−Alder reaction and intramolecular Friedel−Crafts acylation.[21−23]

In this context, we planned to demonstrate the usefulness of our reaction by applying it to *α*-hydroxylation of tetralone-derived *β*-ketoesters. DFT calculation suggested that the *β*-ketoester group in tetralones **5** interacts with guanidinium and urea groups in the catalyst **2**, and the oxidant coordinates with the remainder of the urea group in **2**, then oxidation proceeds from the *si*-face due to the chirality of the catalyst **2** (Figure 3). Based on this TS model, we anticipated that the stereochemistry of the substituents at the *β*- or *γ*-positions in tetralone **5** would affect the reactivity for *α*-hydroxylation (Scheme 1c). Indeed, in DFT calculations of **TS-S** models for *β*- and *γ*-substituted tetralone derivatives, the TS model with *anti* relations (e.g., R^1, R^3) of the electrophilic OH group of CHP and the *β*- or *γ*-substituent is energetically favored over the *syn* structure (e.g., R^2, R^4).[24] These effects are mainly due to weaker steric repulsion between CHP and the *β*- or *γ*-substituent and a more stable flipped conformation of the tetralone core moiety. These computations strongly suggested that the *anti*-products **6A** and **6B** would be

DOI: 10.1021/ja511149y
J. Am. Chem. Soc. 2015, 137, 1909−1915

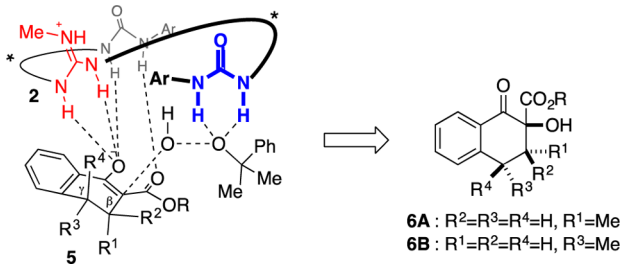

Figure 3. Calculated TS model for oxidative kinetic resolution of β- and γ-substituted tetralone-derived β-ketoesters **5** catalyzed by **2**.

preferentially generated from β- or γ-methyl-substituted tetralones, respectively, in the presence of catalyst **2** and CHP (Figure 3). Based on these insights, we examined the oxidative kinetic resolution of β-ketoesters *rac*-**5** of tetralones bearing substituents at the β- and/or γ-positions to obtain optically active substituted tetralones.

Oxidative kinetic resolution was examined with *rac*-**5a**, bearing a phenyl substituent at the β-position, and catalyst **2** under the previously developed conditions in the presence of CHP (0.5 equiv). First, the catalyst structure was varied, focusing on the chiral spacer part of the R group (Table 1).[25] In the case of the catalyst **2a**, moderate selectivity was observed in kinetic resolution, i.e., the oxidation product **6a** was obtained in 33% yield with 72% ee, and **5a** was recovered in 74% yield, with 38% ee (entry 1). By varying the R group (methyl, isopropyl, and phenyl groups), the selectivity was increased (entries 2−4); in the case of **2d**, **6a** was obtained in 40% yield with 91% ee and **5a** was recovered in 47% yield with 64% ee, and the *s* value was found to be 41 (entry 4). We further optimized the reaction conditions with the catalyst **2d**, and **6a** and **5a** were obtained with 83% ee (49% yield) and 97% ee (42% yield), respectively, by increasing the amount of CHP to 0.75 equiv and prolonging the reaction time to 48 h (entry 5).

With the optimized conditions in hand (Table 1, entry 5), the substrate scope for the oxidative kinetic resolution of β-ketoesters bearing substituents at the β- or γ-position in tetralone structure was investigated (Table 2). In the case of β-substituted tetralones with electron-donating and electron-withdrawing groups on the phenyl group (*rac*-**5b−j**), oxidative kinetic resolution reaction proceeded smoothly, and high enantioselectivities were obtained for both oxidation products **6b−j** (83−90% ee) and recovered **5b−j** (88−99% ee); high *s* values of 43−99 were obtained (Table 2, entries 1−9). The substrate with a 1-naphthyl substituent (*rac*-**5k**) also reacted efficiently, and **6k** and **5k** were obtained in 72% ee and 97% ee, respectively (*s* = 25, Table 2). Moderate reactivities were observed for *rac*-**5l−n** bearing an alkyl or aralkyl group at the β-position, and high selectivities were obtained for oxidation products **6l−n** (86−90% ee) and for **5l−n** (67−74% ee) (entries 11−13). On the other hand, low reactivities were observed for *rac*-**5o** and *rac*-**5p** bearing isopropyl and cyclohexyl groups, with moderate *s* values of 18 and 20, respectively, although good selectivities were still obtained for **6o** (84% ee) and **6p** (83% ee) (entries 14 and 15). In the case of γ-substituted tetralones with phenyl and methyl groups (*rac*-**5q** and *rac*-**5r**), resolution took place efficiently, and high enantioselectivities were obtained for **6q** (89% ee) and **6r** (91% ee) as well as recovered **5q** (99% ee) and **5r** (92% ee), with *s* values of 89 and 69, respectively (entries 16,17).

Synthesis of (+)-linoxepin (13). The newly developed oxidative kinetic resolution method for tetralones was applied to the synthesis of (+)-linoxepin (**13**), which was isolated from *Linum perenne* as a caffeic acid dimer possessing an oxidation-prone dihydronaphthalene structure with a tetrasubstituted double bond embedded in a highly strained dihydrooxepine ring system (Scheme 3).[26,27]

Oxidative kinetic resolution of *rac*-**7** was performed with (*R*,*R*)-**2d** in the presence of CHP (0.75 equiv) in toluene, and (−)-**7** was obtained in 37% yield with 99% ee, together with (+)-**8** in 52% yield with 77% ee. Then, synthesis of (+)-linoxepin (**13**) from (−)-**7** was examined. The reaction of (−)-**7** with triflic anhydride in the presence of sodium hydride gave vinyl triflate **9**, which was subjected to Suzuki−Miyaura coupling reaction with boron reagent **10** in the presence of $Pd(PPh_3)_4$. The TBS group was removed, and lactonization was performed with 4 M HCl in methanol. Then, benzyl group was removed under hydrogenolysis conditions catalyzed by palladium on carbon to give diol **12**. Compound **12** was reacted with diethyl azodicarboxylate (DEAD) in the presence of triphenyl phosphine to construct the dihydrooxepine ring, affording (+)-linoxepin (**13**) in 88% yield.

Table 1. Optimization of the Reaction Conditions[a]

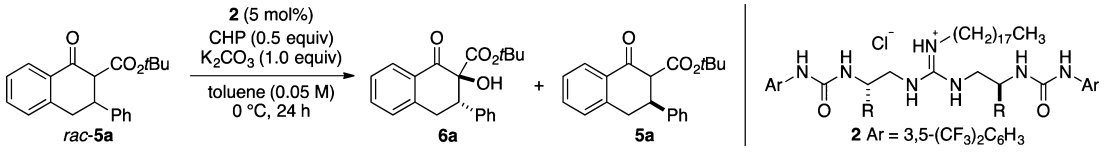

entry	cat.		6a		5a		
		R	yield [%][b]	ee [%][c]	yield [%][d]	ee [%][c]	*s* value[e]
1	**2a**	Bn	33	72	74	38	9
2	**2b**	Me	10	11	81	1	1
3	**2c**	*i*Pr	20	64	56	18	5
4	**2d**	Ph	40	91	47	64	41
5[f]	**2d**	Ph	49	83	42	97	44

[a]Reaction conditions: *rac*-**5a** (0.05 mmol), CHP (0.025 mmol) and K_2CO_3 (0.05 mmol) in the presence of **2** (5 mol %) in toluene (1.0 mL) at 0 °C for 24 h. [b]Determined by ^{1}H NMR spectroscopy with isopropyl alcohol as an internal standard. [c]Determined by HPLC analysis using a chiral stationary phase. [d]Yield of isolated product. [e]The selectivity factor (*s* value) was calculated as follows: *s* value = k_{fast}/k_{slow} = ln[1 − *C*(1 + ee**6**)]/ln[1 − *C*(1 − ee**6**)] = ln[(1 − *C*)(1 − ee**5**)]/ln[(1 − *C*)(1 + ee**5**)]; *C* = ee**5**/(ee**5** + ee**6**). [f]The reaction was run with *rac*-**5a** (0.05 mmol), CHP (0.038 mmol, 0.75 equiv), and K_2CO_3 (0.05 mmol, 1.0 equiv) in the presence of **3d** (5 mol %) in toluene (1.5 mL, 0.03 M) at 0 °C for 48 h. CHP = cumene hydroperoxide.

DOI: 10.1021/ja511149y
J. Am. Chem. Soc. 2015, 137, 1909−1915

Table 2. Oxidative Kinetic Resolution of β- or γ-Substituted Tetralone Derivatives[a]

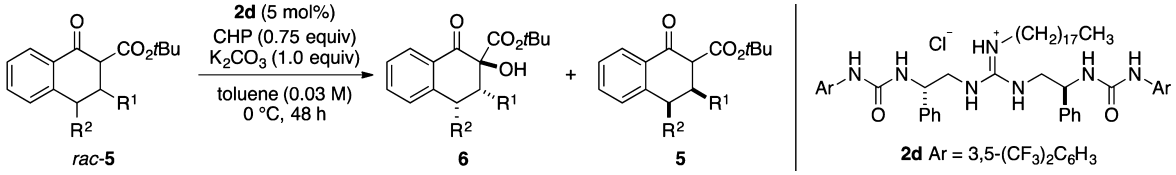

entry	rac-5	R^1	R^2	6 yield [%][b]	6 ee [%][c]	5 yield [%][b]	5 ee [%][c]	s value[d]
1	rac-**5b**	2-Cl-C_6H_5	H	50 (**6b**)	90	44 (**5b**)	94	43
2	rac-**5c**	3-Cl-C_6H_5	H	47 (**6c**)	89	46 (**5c**)	88	50
3	rac-**5d**	4-Cl-C_6H_5	H	45 (**6d**)	87	44 (**5d**)	93	48
4	rac-**5e**	2-CF_3−C_6H_5	H	50 (**6e**)	90	43 (**5e**)	99	99
5	rac-**5f**	2-MeO-C_6H_5	H	44 (**6f**)	88	42 (**5f**)	90	48
6	rac-**5g**	3-MeO-C_6H_5	H	48 (**6g**)	89	44 (**5g**)	89	51
7	rac-**5h**	4-MeO-C_6H_5	H	46 (**6h**)	83	43 (**5h**)	99	56
8	rac-**5i**	4-Me-C_6H_5	H	48 (**6i**)	84	43 (**5i**)	94	40
9	rac-**5j**	3,5-MeO-C_6H_4	H	42 (**6j**)	89	44 (**5j**)	90	52
10	rac-**5k**	1-naphtyl	H	55 (**6k**)	72	40 (**5k**)	97	25
11	rac-**5l**	Me	H	43 (**6l**)	90	43 (**5l**)	67	38
12	rac-**5m**	*n*Pr	H	44 (**6m**)	86	44 (**5m**)	70	28
13	rac-**5n**	CH_2CH_2Ph	H	45 (**6n**)	88	42 (**5n**)	74	34
14[e]	rac-**5o**	*i*Pr	H	34 (**6o**)	84	61 (**5o**)	47	18
15[e]	rac-**5p**	cyclohexyl	H	37 (**6p**)	83	53 (**5p**)	61	20
16	rac-**5q**	H	Ph	51 (**6q**)	89	44 (**5q**)	99	89
17	rac-**5r**	H	Me	48 (**6r**)	91	45 (**5r**)	92	69

[a]Reaction conditions: rac-**5** (0.05 mmol), CHP (0.038 mmol) and K_2CO_3 (0.05 mmol) in the presence of **2d** (5 mol %) in toluene (1.5 mL) at 0 °C for 48 h. [b]Yield of isolated product. [c]Determined by HPLC analysis using a chiral stationary phase after decarboxylation under acidic conditions. [d]The selectivity factor (*s* value) was calculated as follows: s value = k_{fast}/k_{slow} = In[1 − C(1 + ee**6**)]/In[1 − C(1 − ee**6**)] = In[(1 − C)(1 − ee**5**)]/In[(1 − C)(1 + ee**5**)]; C = ee**5**/(ee**5** + ee**6**). [e]The reaction was run with 1.5 equiv of CHP.

Scheme 3. Synthesis of (+)-Linoxepin (13)[a]

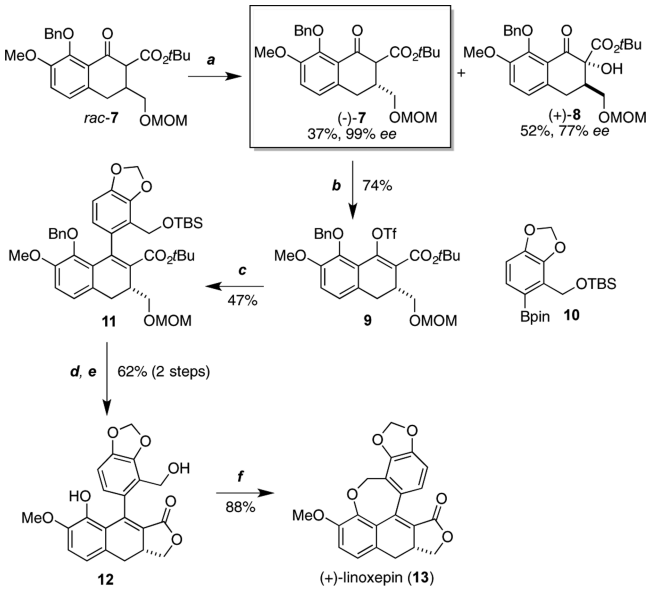

[a]Reagents and conditions: (a) (*R*,*R*)-**2d** (5 mol %), CHP (0.75 equiv), K_2CO_3 (1.0 equiv), toluene, 0 °C, 72 h ((−)-**7**: 37%, 99% ee) ((+)-**8**: 52%, 77% ee); (b) Tf_2O (1.2 equiv), NaH (2.0 equiv), Et_2O, 0 °C to RT, 0.5 h (74%); (c) **10** (1.2 equiv), $Pd(PPh_3)_4$ (5 mol %), KOH (5.0 equiv), 1,4-dioxane, 60 °C, 1 h (47%); (d) 4 M HCl/MeOH, RT, 3 h; (e) H_2 (balloon), Pd/C (10 wt %), MeOH, RT, 0.5 h (62%, 2 steps); (f) DEAD (4.0 equiv), PPh_3 (4.0 equiv), THF, 0 °C to RT, 0.5 h (88%). CHP = cumen hydroperoxide, DEAD = diethyl azodicarboxylate, THF = tetrahydrofuran.

CONCLUSIONS

DFT calculations were done to uncover the mechanism of the highly enantioselective α-hydroxylation of tetralone-derived β-ketoesters in the presence of structurally flexible guanidine-bisurea bifunctional organocatalyst. The identified TS structure indicated that the β-ketoester group of tetralone interacts with guanidine and urea groups in the catalyst **2d**, and oxidant coordinates with the remainder of the urea group. The oxidation then proceeds from the *si*-face owing to the chirality of the catalyst. Based on the insights provided by this TS model, we designed novel methodology for asymmetric synthesis of β- and/or γ-substituted tetralones by oxidative kinetic resolution reaction of tetralone-derived β-ketoesters, using guanidine-urea bifunctional organocatalyst **2d** and CHP. The kinetic resolution reaction of various tetralone derivatives proceeded with high selectivity; the selectivity factor (*s* value) reached 99. This reaction was successfully applied to the synthesis of (+)-linoxepin (**13**) in 6 steps from tetralone *rac*-**7**. We expect that it will also be applicable to the synthesis of other natural products.

ASSOCIATED CONTENT

Supporting Information

Experimental details and characterization. This material is available free of charge via the Internet at http://pubs.acs.org.

AUTHOR INFORMATION

Corresponding Author

*knaga@cc.tuat.ac.jp

Notes

The authors declare no competing financial interest.

DOI: 10.1021/ja511149y
J. Am. Chem. Soc. 2015, 137, 1909−1915

■ ACKNOWLEDGMENTS

We would like to dedicate this article to celebrate the 20th anniversary of the Department of Biotechnology and Life Science at Tokyo University of Agriculture and Technology. This work was supported by a Grant-in-Aid for Scientific Research on Innovative Areas "Advanced Molecular Transformations by Organocatalysts" (nos. 23105013 and 23105005) from The Ministry of Education, Culture, Sports, Science and Technology, Japan and MEXT-Supported Program for the Strategic Research Foundation at Private Universities. M.O. was the recipient of a Sasakawa Scientific Research Grant from The Japan Science Society.

■ REFERENCES

(1) (a) Sohtome, Y.; Hashimoto, Y.; Nagasawa, K. *Eur. J. Org. Chem.* **2006**, 2894−2897. (d) Takada, K.; Nagasawa, K. *Adv. Synth. Catal.* **2009**, *351*, 345−347. (e) Takada, K.; Tanaka, S.; Nagasawa, K. *Synlett* **2009**, 1643−1646. (f) Sohtome, Y.; Shin, B.; Horitsugi, N.; Takagi, R.; Noguchi, K.; Nagasawa, K. *Angew. Chem., Int. Ed.* **2010**, *49*, 7299−7303. (g) Sohtome, Y.; Tanaka, S.; Takada, K.; Yamaguchi, T.; Noguchi, K.; Nagasawa, K. *Angew. Chem., Int. Ed.* **2010**, *49*, 9254−9257. (h) Sohtome, Y.; Shin, B.; Horitsugi, N.; Noguchi, K.; Nagsawa, K. *Chem.—Asian J.* **2011**, *6*, 2463−2470. (i) Sohtome, Y.; Yamaguchi, T.; Shin, B.; Nagasawa, K. *Chem. Lett.* **2011**, *40*, 843−845.

(2) Odagi, M.; Furukori, K.; Watanabe, T.; Nagasawa, K. *Chem.—Eur. J.* **2013**, *19*, 16740−16745.

(3) For reviews of computational studies of organocatalysis, see: (a) Cheong, P. H-Y.; Legault, C. Y.; Um, J. M.; Çelebi-Ölçüm, N.; Houk, K. N. *Chem. Rev.* **2011**, *111*, 5042−5137.

(4) Becke, A. D. *J. Chem. Phys.* **1993**, *98*, 5648−5652. (b) Lee, C.; Yang, W.; Parr, R. G. *Phys. Rev. B* **1988**, *37*, 785−789.

(5) Zhao, Y.; Schultz, N. E.; Truhlar, D. G. *J. Chem. Theory Comput.* **2006**, *2*, 364−382.

(6) Hehre, W. J.; Radom, L.; Schleyer, P. v. R.; Pople, J. A. *Ab initio Molecular Orbital Theory*; Wiley: New York, 1986, and references cited therein.

(7) Frisch, M. J.; Trucks, G. W.; Schlegel, H. B.; Scuseria, G. E.; Robb, M. A.; Cheeseman, J. R.; Scalmani, G.; Barone, V.; Mennucci, B.; Petersson, G. A.; Nakatsuji, H.; Caricato, M.; Li, X.; Hratchian, H. P.; Izmaylov, A. F.; Bloino, J.; Zheng, G.; Sonnenberg, J. L.; Hada, M.; Ehara, M.; Toyota, K.; Fukuda, R.; Hasegawa, J.; Ishida, M.; Nakajima, T.; Honda, Y.; Kitao, O.; Nakai, H.; Vreven, T.; Montgomery, J. A., Jr.; Peralta, J. E.; Ogliaro, F.; Bearpark, M.; Heyd, J. J.; Brothers, E.; Kudin, K. N.; Staroverov, V. N.; Keith, T.; Kobayashi, R.; Normand, J.; Raghavachari, K.; Rendell, A.; Burant, J. C.; Iyengar, S. S.; Tomasi, J.; Cossi, M.; Rega, N.; Millam, J. M.; Klene, M.; Knox, J. E.; Cross, J. B.; Bakken, V.; Adamo, C.; Jaramillo, J.; Gomperts, R.; Stratmann, R. E.; Yazyev, O.; Austin, A. J.; Cammi, R.; Pomelli, C.; Ochterski, J. W.; Martin, R. L.; Morokuma, K.; Zakrzewski, V. G.; Voth, G. A.; Salvador, P.; Dannenberg, J. J.; Dapprich, S.; Daniels, A. D.; Farkas, O.; Foresman, J. B.; Ortiz, J. V.; Cioslowski, J.; and Fox, D. J. *Gaussian 09*, revision D.01; Gaussian, Inc.: Wallingford, CT, 2013.

(8) Computational details using simplified chemical models are shown in Supporting Information. Various activation modes of enolate and CHP with guanidine and urea groups were also described (see S-36−39).

(9) To reduce the computational cost, the calculation was done for a methyl group instead of an *n*-octadecalyl group on the guanidinium moiety as a realistic chemical model. Various TS conformations are shown in the Supporting Information.

(10) **TS-S** and **TS-R** were defined as the transition states generating *S* and *R* stereochemistry at C2 in **4**, respectively.

(11) (a) Hamza, A.; Schubert, G.; Soós, T.; Pápai, I. *J. Am. Chem. Soc.* **2006**, *128*, 13151−13160. (b) Zhu, R.; Zhang, D.; Wu, J.; Liu, C. *Tetrahedron: Asymmetry* **2006**, *17*, 1611−1616. (c) Zhang, D.; Wang, G.; Zhu, R. *Tetrahedron: Asymmetry* **2008**, *19*, 568−576. (d) Chen, D.; Lu, N.; Zhang, G.; Mi, S. *Tetrahedron: Asymmetry* **2009**, *20*, 1365−1368. (e) Zuend, S. J.; Jacobsen, E. N. *J. Am. Chem. Soc.* **2009**, *131*, 15358−15374. (f) Almas-i, D.; Alonso, D. A.; Gómez-Bengoa, E.; Nájera, C. *J. Org. Chem.* **2009**, *74*, 6163−6168. (g) Uyeda, C.; Rötheli, A. R.; Jacobsen, E. N. *Angew. Chem., Int. Ed.* **2010**, *49*, 9753−9756. (h) Uyeda, C.; Jacobsen, E. N. *J. Am. Chem. Soc.* **2011**, *133*, 5062−5075. (i) Zhu, J.-L.; Zhang, Y.; Liu, C.; Zheng, A.-M.; Wang, W. *J. Org. Chem.* **2012**, *77*, 9813−9825. (j) Shubina, T. E.; Freund, M.; Schenker, S.; Clark, T.; Tsogoeva, S. B. *Beilstein J. Org. Chem.* **2012**, *8*, 1485−1498. (k) Gómez-Torres, E.; Alonso, D. A.; Gómez-Bengoa, E.; Nájera, C. *Eur. J. Org. Chem.* **2013**, 1434−1440. (l) Azuma, T.; Kobayashi, Y.; Sakata, K.; Sasamori, T.; Tokitoh, N.; Takemoto, Y. *J. Org. Chem.* **2014**, *79*, 1805−1817. (m) Kótai, B.; Kardos, G.; Hamza, A.; Farkas, V.; Pápai, I.; Soós, T. *Chem.—Eur. J.* **2014**, *20*, 5631−5639.

(12) The energies of **TS-S** and **TS-R** were dissected into the distortion (E_{dist}) and interaction energies (E_{int}) for the two distorted fragments (catalyst and substrates) constructing TS. The differences for each energy (ΔE_{dist} and ΔE_{int}) between **TS-S** and **TS-R** were calculated by the counterpoise method. The computational details are shown in Supporting Information. The original distortion/interaction analysis, see: (a) Morokuma, K.; Kitaura, K. I *Chemical Applications of Atomic and Molecular Electrostatic Potentials*; Politzer, P., Truhlar, D. G., Eds.; Plenum: New York, 1981. (b) Ess, D. N.; Houk, K. N. *J. Am. Chem. Soc.* **2007**, *129*, 10646−10647. (c) Ess, D. H.; Houk, K. N. *J. Am. Chem. Soc.* **2008**, *130*, 10187−10198. (d) Lam, Y.-H.; Cheong, P. H.-Y.; Blasco Mata, J. M.; Stanway, S. J.; Gouverneur, V. R.; Houk, K. N. *J. Am. Chem. Soc.* **2009**, *131*, 1947−1957. (e) Paton, R. S.; Kim, S.; Ross, A. G.; Danishefsky, S. J.; Houk, K. N. *Angew. Chem., Int. Ed.* **2011**, *50*, 10366−10368. (f) Green, A. G.; Liu, P.; Merlic, C. A.; Houk, K. N. *J. Am. Chem. Soc.* **2014**, *136*, 4575−4583.

(13) The negative charge distribution on ketone carbonyl and ester carbonyl in the *β*-ketoester enolate was confirmed by natural population analysis to be −0.686 and −0.678, respectively.

(14) See Supporting Information for structural details of the TS models.

(15) For reviews on asymmetric michael reaction and vinylogous aldol reaction, see: (a) Rossiter, B. E.; Swingle, N. M. *Chem. Rev.* **1992**, *92*, 771−806. (b) Hawner, C.; Alexakis, A. *Chem. Commun.* **2010**, *46*, 7295−7306. (c) Denmark, S. E.; Heemstra, J. R., Jr.; Beutner, G. L. *Angew. Chem., Int. Ed.* **2005**, *44*, 4682−4698.

(16) Biologically active natural products containing *β*- and/or *γ*-substituted tetralone core, see: (a) Oka, M.; Kamei, H.; Hamagishi, Y.; Tomita, K.; Miyaki, T.; Konishi, M.; Oki, T. *J. Antibiot.* **1990**, *43*, 967−976. (b) Wellington, K. D.; Cambie, R. C.; Rutledge, P. S.; Bergquist, P. R. *J. Nat. Prod.* **2000**, *63*, 79−85. (c) Laurent, D.; Guella, G.; Mancini, I.; Roquebert, M. F.; Farinole, F.; Pietra, F. *Tetrahedrone* **2002**, *58*, 9163−9167. (d) Wang, K. W.; Mao, J. S.; Tai, Y. P.; Pan, Y. J. *Bioorg. Med. Chem. Lett.* **2006**, *16*, 2274−2277. (e) Cueva, J. P.; Godoy, A. G.; Juncosa, J. I.; Vidi, P. A.; Lill, M. A.; Watts, V. J.; Nichols, D. E. *J. Med. Chem.* **2011**, *54*, 5508−5521. (f) Devkota, K. P.; Covell, D.; Ransom, T.; McMahon, J. B.; Beutler, J. A. *J. Nat. Prod.* **2013**, *76*, 710−714. (g) Izawa, M.; Kimata, S.; Maeda, A.; Kawasaki, T.; Hayakawa, Y. *J. Antibiot.* **2014**, *67*, 159−162.

(17) (a) Fieser, L. F.; Dunn, J. T. *J. Am. Chem. Soc.* **1936**, *58*, 572−575. (b) Engman, L. *Tetrahedron Lett.* **1985**, *26*, 6385−6388. (c) Engman, L. *J. Org. Chem.* **1988**, *53*, 4031−4037. (d) Vargas, A. C.; Martin, I. P.; Sire, B. Q.; Zard, S. Z. *Org. Biomol. Chem.* **2004**, *2*, 3018−3025. (e) Cui, L. Q.; Dong, Z. L.; Liu, K.; Zhang, C. *Org. Lett.* **2011**, *13*, 6488−6491. (f) Yang, T. F.; Wang, K. Y.; Li, H. W.; Tseng, Y. C.; Lien, T. C. *Tetrahedron Lett.* **2012**, *53*, 585−588.

(18) Enzymatic kinetic resolution of 1-tetralones, see: (a) Kasai, M.; Ziffer, H.; Silverton, J. V. *Can. J. Chem.* **1985**, *63*, 1287−1291. (b) Caro, Y.; Torrado, M. A.; Masaguer, C. F.; Raviña, E.; Padın, F.; Brea, J.; Loza, M. A. I. *Bioorg. Med. Chem. lett.* **2004**, *14*, 585−589. (c) Ros, A.; Magriz, A.; Dietrich, H.; Fernandez, R.; Alvarez, E.; Lassaletta, J. M. *Org. Lett.* **2006**, *8*, 127−130. (d) Ding, Z.; Yang, J.; Wang, T.; Shen, Z.; Zhang, Y. *Chem. Commun.* **2009**, 571−573.

(19) Catalytic nonenzymatic kinetic resolution of 1-tetralones, see: (a) Genêt, J. P.; Pfister, X.; Vidal, V. R.; Pinel, C.; Laffitte, J. A. *Tetrahedron Lett.* **1994**, *35*, 4559−4562. (b) Sugi, K. D.; Nagata, T.;

DOI: 10.1021/ja511149y
J. Am. Chem. Soc. 2015, 137, 1909−1915

Yamada, T.; Mukaiyama, T. *Chem. Lett.* **1996**, 1081−1082. (c) Caro, Y.; Torrado, M. A.; Masaguer, C. F.; Raviña, E. *Tetrahedron: Asymmetry* **2003**, *14*, 3689−3696. (d) Ros, A.; Magriz, A.; Dietrich, H.; Fernandez, R.; Alvarez, E.; Lassaletta, J. M. *Org. Lett.* **2006**, *8*, 127−130. (e) Ding, Z.; Yang, J.; Wang, T.; Shen, Z.; Zhang, Y. *Chem. Commun.* **2009**, 571−573.

(20) Manoni, F.; Connon, S. J. *Angew. Chem., Int. Ed.* **2014**, *53*, 2628−2632.

(21) For selected papers on synthesis of racemic β- and/or γ-substituted tetralones using Diels−Alder reaction, see: (a) Nicolaou, K. C.; Gray, D. L.; Tae, J. *J. Am. Chem. Soc.* **2004**, *126*, 613−627. (b) Ting, C. P.; Maimone, T. J. *Angew. Chem., Int. Ed.* **2014**, *53*, 3115−3119.

(22) Synthesis of racemic β- and/or γ-substituted tetralones using intramolecular Friedel−Crafts approach, see: (a) Yang, F. Z.; Trost, M. K.; Fristad, W. E. *Tetrahedron Lett.* **1987**, *28*, 1493−1496. (b) Esteban, G.; López-Sánchez, M. A.; Martínez, M.; Plumet, J. *Tetrahedron* **1998**, *54*, 197−212. (c) Pita, B.; Masaguer, C. F.; Ravina, E. *Tetrahedron Lett.* **2002**, *43*, 7929−7932. (d) Cui, D. M.; Kawamura, M.; Shimada, S.; Hayashi, T.; Tanaka, M. *Tetrahedron Lett.* **2003**, *44*, 4007−4010. (e) Prakash, G. K. S.; Yan, P.; Torok, B.; Olah, G. A. *Catal. Lett.* **2003**, *87*, 109−112. (f) Zhang, L.; Kozmin, S. A. *J. Am. Chem. Soc.* **2004**, *126*, 10204−10205. (g) Fillion, E.; Fishlock, D.; Wilsily, A.; Goll, J. M. *J. Org. Chem.* **2005**, *70*, 1316−1327.

(23) Synthesis of optically active β- and/or γ-substituted tetralones in total synthesis of natural products, see: (a) White, J. D.; Hrnciar, P.; Stappenbeck, F. *J. Org. Chem.* **1997**, *62*, 5250−5251. (b) Elford, T. G.; Nave, S.; Sonawane, R. P.; Aggarwal, V. K. *J. Am. Chem. Soc.* **2011**, *133*, 16798−16801. (c) Reddel, J. C.; Lutz, K. E.; Diagne, A. B.; Thomson, R. J. *Angew. Chem., Int. Ed.* **2014**, *53*, 1395−1398.

(24) See Supporting Information for details of the computational calculation of **TS-S** models for β- and γ-substituted tetralone derivatives.

(25) Absolute configurations were determined by X-ray crystallography. See supporting information for details. CCDC 1018477 (*p*-BrBz **6k**) and 1018478 (*p*-BrBz **6q**) contains the supplementary crystallographic data for this paper. These data can be obtained free of charge from The Cambridge Crystallographic Data Centre via www.ccdc.cam.ac.uk/data_request/cif.

(26) Schmidt, T. J.; Vossing, S.; Klaes, M.; Grimme, S. *Planta Med.* **2007**, *73*, 1574−1580.

(27) Total synthesis of linoxepin, see: (a) Tietze, L. F.; Duefert, S. C.; Clerc, J.; Bischoff, M.; Maass, C.; Stalke, D. *Angew. Chem., Int. Ed.* **2013**, *52*, 3191−3194. (b) Weinstabl, H.; Suhartono, M.; Qureshi, Z.; Lautens, M. *Angew. Chem., Int. Ed.* **2013**, *52*, 5305−5308. (c) Qureshi, Z.; Weinstabl, H.; Suhartono, M.; Liu, H.; Thesmar, P.; Lautens, M. *Eur. J. Org. Chem.* **2014**, 4053−4069. (d) Tietze, L. F.; Clerc, J.; Biller, S.; Duefert, S. C.; Bischoff, M. *Chem.—Eur. J.* **2014**, *20*, 17119−17124.

DOI: 10.1021/ja511149y
J. Am. Chem. Soc. 2015, 137, 1909−1915